Influence Analysis on the Bearings' Impedance Behavior of Inverter-Fed Motor Drives

Silvan Scheuermann, Dr. Björn Hagemann, Dr. Matthias Brodatzki, Prof. Dr.-Ing Martin Doppelbauer
Institute of Electrical Engineering (ETI) – Karlsruhe Institute of Technology (KIT), Karlsruhe, Germany
silvan.scheuermann@kit.edu

Abstract

The present paper reveals many crucial influences on the bearings' behavior under electrical high-frequency excitation and helps to understand the phenomena of electric damage in bearings. Such bearing damages are often seen in inverter-fed drives. The use of fast-switching power inverters with SiC or GaN semiconductor technologies amplifies and increases the likelihood of such damage. This study describes an influence analysis on the impedance behavior of bearings deployed in inverter-fed drives. In the author's previous publication [1], a novel approach for an experimental setup to determine the electric impedance of bearings for traction applications is presented. Based on this test bench, the results of the influence on the investigated parameters such as variations in speed, radial and axial loads, or different types of oil and material of the bearings' retainer are shown in the present paper.

1 Introduction

Today's electric machines, not only traction motors, are mainly fed by variable-speed inverter systems. The use of new semiconductor materials, such as SiC or GaN amplifies the effect of switching transients due to square-wave pulses with steep and high voltage edges. In literature, the electrical impedance of bearings has often been investigated to determine and to characterize the lubrication type or the film thickness of the elasto-hydrodynamic (EHD) contact between the rolling elements [2-4]. Further research investigates the occurrence of bearing currents and other erosive effects in such contacts. The capacitances in the bearings between the inner and outer raceways create a voltage divider proportional to the common-mode voltage at the motors' terminal [5]. The capacitive voltage divider, representational in **Figure 3**, also known as the Bearing Voltage Ratio (BVR) in **Formula (1)** represents the ratio between the bearing voltage U_b and the common mode voltage U_CM at the motors' terminal. The BVR can be calculated by dividing the winding-to-rotor capacitance C_wr by the sum of the stator-to-rotor capacitance C_sr, the bearings' capacitances of the drive- ($C_\mathrm{b,DE}$) and non-drive-end ($C_\mathrm{b,NDE}$) and the winding-to-rotor capacitance C_wr.

$$BVR = \frac{U_\mathrm{b}}{U_\mathrm{CM}} = \frac{C_\mathrm{wr}}{C_\mathrm{b,DE} + C_\mathrm{wr} + C_\mathrm{sr} + C_\mathrm{b,NDE}} \tag{1}$$

Breakdowns of the capacitances and electric discharges in the bearings' lubrication can lead to a meltdown or vaporization of the material of the bearings' rings or lubrication. Damage and failure of the motors are just the consequence and are further indicated by pittings or corrugated patterns on the raceways (**Figure 1, 2**).

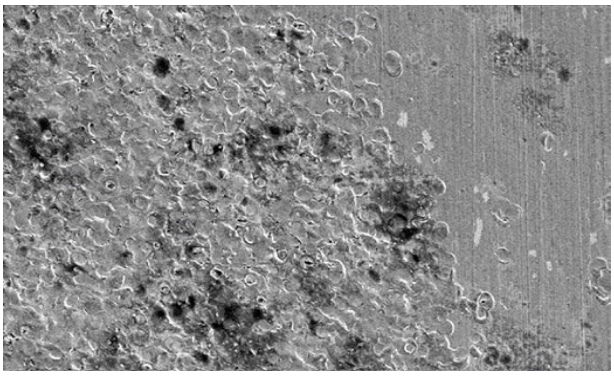

Figure 1: Pittings on a bearings' raceway [2]

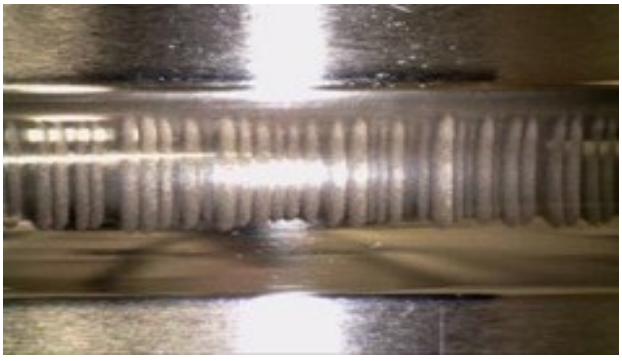

Figure 2: Corrugated patterns at the outer raceway

2 Fundamentals

2.1 Analytical characterization of the rolling bearings' capacitance

In literature, it is common to characterize rolling bearings under EHD – conditions by treating each rolling element as a single capacitor and summing up their contributions. The

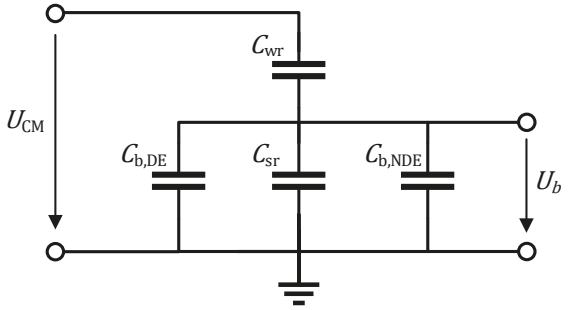

Figure 3: Bearing Voltage Ratio (BVR)

Hertzian contact surface A_{Hertz} forms an analogy of a plate capacitor between the rolling element and the raceways. The Hertzian factor k_{Hertz} is dimensionless and depends on the geometry of the contact. It is used to calculate the contact pressure distribution and the maximum contact stress between two bodies. The thickness of the lubricating film h_0, which describes the distance between these figurative plates, influences the magnitude of the capacity dominantly. Besides, the permittivity ε_r of the lubrication, which can change due to a variation in pressure or temperature [7] influences the capacitance further. In [5], the Hertzian capacitance of the bearings is calculated by

$$C_{\mathrm{Hertz}} = k_{\mathrm{Hertz}} \varepsilon_0 \varepsilon_{\mathrm{r}} \frac{A_{\mathrm{Hertz}}}{h_0}. \tag{2}$$

Hamrock and Dowson [6] calculate the lubricant film thickness $h_0$in each rolling contact by (3).

$$h_0 = 2.69 \cdot r_{\mathrm{x}} \cdot (1 - 0{,}61 \cdot e^{-0{,}73 \cdot k}) \cdot \bar{U}_{\mathrm{r}}^{0.67} \cdot (\alpha \cdot E')^{0.53} \cdot \bar{W}^{-0.067} \tag{3}$$

The lubrication film thickness h_0 depends not only on the load or pressure of each rolling element but also geometric quantities like the curvature radius r_{x} and material properties, e.g. the combined Young's Modulus E' influences the calculation. The ellipticity factor k describes the relationship between the large and small half-axis of the balls' pressure ellipse, while $\bar{\mathrm{U}}_{\mathrm{r}}$ represents the dimensionless velocity and $\bar{\mathrm{W}}$ the dimensionless load of one rolling element. α describes the viscosity-pressure coefficient of the lubricant and the combined Youngs' Modulus E' is defined by the Youngs' Modulus E and Poisson number ν of the bearings' steel. Finally, the whole bearing's capacitance is calculated as the combination of the inner-raceway capacitances C_{i} and the outer-ring capacitance C_{o} of each rolling element by **Formula (4)** as in [5].

$$C_{\mathrm{b}} = \frac{\Sigma_{N_{\mathrm{WK}}} C_{\mathrm{i},k} \cdot \Sigma_{N_{\mathrm{WK}}} C_{\mathrm{o},k}}{k_{\mathrm{s}} \cdot (\Sigma_{N_{\mathrm{WK}}} C_{\mathrm{i},k} + \Sigma_{N_{\mathrm{WK}}} C_{\mathrm{o},k})} \tag{4}$$

2.2 Measurement setup

Figure 4 shows the newly developed test setup for bearings. In the author's previous publication [1], the bearing test bench is explained in detail.

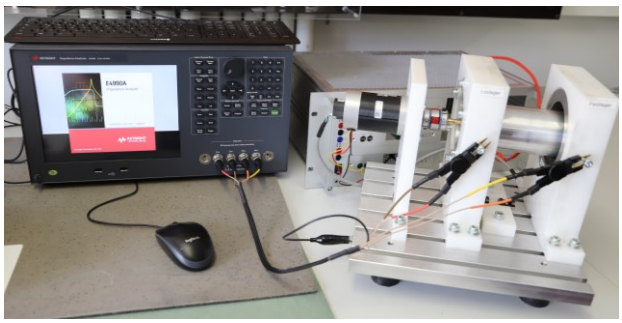

Figure 4: Measurement setup to determine the bearings impedance

In summary, the test bench consists of a motor, which is connected by an insulating elastomer coupling to the main shaft. On this shaft, the bearings of the types SKF 6011 and SKF 61813 are load-carrying. For further separation of all noisy signals from the impedance analyzer, the bearings are press-fitted into a bushing approach and further, these are inserted into brackets made of non-conducting polyoxymethylene (POM). The bushing approach is beneficial because it is easily possible to exchange the bearings or the bearings' sizes. Since those are made of aluminium, they are used as connection terminals to the impedance analyzer. In the middle between the two bearings, a little roller is arranged, which can provide external radial forces. It is connected to a load cell to measure those forces. Besides, a preload washer with a well-known load-displacement characteristic is used to provide axial loads. For the temperature monitioring, Type K temperature sensors are attached to the oil and outer rings of the bearings. Further, a thermographic camera can measure the temperatures of the different components. The Keysight E4990A impedance analyzer on the left-hand side in **Figure 4** is provided to measure the impedance behavior of the bearings between 10 kHz and 5 MHz under the different operation conditions.

2.3 Properties and specifications of the investigated variations

The two single-row ball bearings of the types SKF 6011 [6] and SKF 61813 [7] were chosen because of their versatility and use in automotive traction applications. Further, they have low friction and are optimized for low noise and low vibration, which enables high rotational speeds. They withstand radial and axial loads in both directions, are easy to mount, and require less maintenance than many other bearing types [6, 7]. The properties and specifications are shown in **Table 1**, based on the information in [6-11].

Property	**SKF 6011**	**SKF 61813**
Number of balls N_{WK}	13	24
Radius of inner race curvature r_{in}	31.07 mm	34.72 mm
Radius of inner race r_{i}	5.37 mm	2.848 mm
Radius of balls r_{WK}	5.16 mm	2.778 mm
E-modulus E	208000 MPa [9]	
Poisson number ϑ	0.3 [9]	
Load of each bearing W_{max}	7 N	
Viscosity-pressure coefficient α	2.3e-8 N^{-1} [9]	

Table 1: Specifications of the investigated bearings

The ball bearings' retainer is either made of metal or polymer. For the influence analysis with regard to the oil type variation on the bearings' capacitances, three different sprayable lubricants have been investigated. Besides, three typical bearing lubricants, which are either grease, liquid grease, or an automatic transmission fluid (ATF) for automotive applications, was employed. The details and further specifications can be found in **Table 2**, or in the respective data sheets [8-11].

The variation in speed was varied in the range between 100 and 5000 rpm. The axial load variation ranges between no axial preload and 3.5 mm deflection, which is equal to an axial load of 400 N. The radial load swept up to 600 N.

Lubricant	Category	Density	Kinematic viscosity
Würth HHS 2000	Oil	0.742 $g\ cm^{-3}$	> 20 $mm^2\ s^{-1}$
Würth HHS Fluid	Viscous grease	0.773 $g\ cm^{-3}$	> 25 $mm^2\ s^{-1}$
Würth HHS Lube	Grease	0.78 $g\ cm^{-3}$	-
Shell S6 ATF D971	Oil	0.822 g cm^{-3}	18 $mm^2\ s^{-1}$

Table 2: Specifications of the investigated lubricants

3 Measurements

In general, a prediction for the capacitance of the bearings or also the lubrication condition can be made by measuring the impedance. Since the impedance type within a bearing changes from resistive to capacitive when a lubrication film builds up, this transition must be seen also in the impedance behavior of the respective bearing under test. In the following, the bearings' measurement results are presented. By changing the speed, load and the bearings' retainer or lubricantion type systematically, the operational factors affecting the bearings can be understood and sources of damage might be identified.

3.1 Arrangement

Since a motor can consist of different bearing types at the drive- and non-drive end, also two different bearings were mounted on the test bench. As **Figure 5** indicates, the capacitance of the floating bearing $C_{\mathrm{DE},n}$ is much lower compared to the fixed bearing $C_{\mathrm{NDE},n}$.

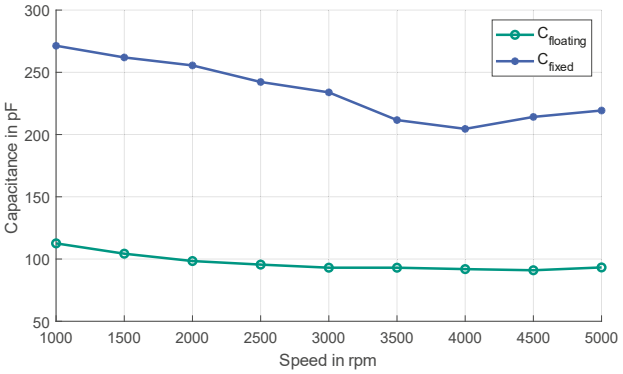

Figure 5: Measurement of the capacitance of the floating bearing $C_{DE,n}$ and fixed bearing $C_{DE,n}$ in parallel

This behavior remains constant over the whole speed range up to 5000 rpm. Below the speed of 100 rpm for the SKF 6011 bearing no capacitance can be measured, while the SKF 61813 bearing requires at least a speed of 200 rpm to build up a separating lubrication film.

The curves for the floating bearing are generally at a lower level due to the higher number of balls. A FE analysis in [1] confirms that the number of balls in the bearing must be the cause for this effect.

Thanks to the series arrangement of the bearings on the test bench's main shaft, the bearings can be either measured in parallel between the bearings' outer ring and the main shaft or in series. If one deploys an analytical series arrangement approach of capacitors, the total capacitance is reduced compared to the individual capacitances. This is because the effective capacitance in a series combination is inversely proportional to the sum of the reciprocals of the individual capacitances. **Figure 6** shows the curves for the mathematical calculation and the measurement result of the series arrangement. Since it matches almost exactly with the analytical calculation with **Formula (5),** the series arrangement of two bearings of different types is validated.

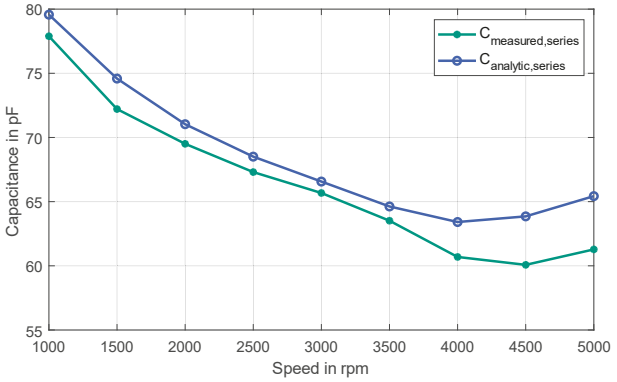

Figure 6: Measurement and mathematical modelling of the series arrangement of two different bearings

$$C_{\mathrm{b,series},n} = \frac{C_{\mathrm{NDE},n} \cdot C_{\mathrm{DE},n}}{C_{\mathrm{NDE},n} + C_{\mathrm{DE},n}} \qquad (5)$$

3.2 Retainer's influence

A bearings' retainer is carrying the rolling elements of a bearing. The retainer ensures the distance of the rolling

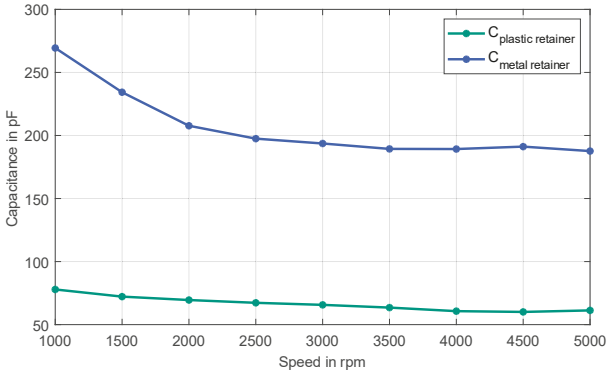

Figure 7: Measurement of the capacitances of the bearings with either plastic or metal retainer

elements on its raceway, so that they do not touch or rub against each other. Further, it establishes an even load distribution of the rolling elements in the bearing. The material of the retainer can be made of any metal or also polymer. **Figure 7** indicates that the bearings' cage made of metal has a much higher capacitance than the ones, equipped with polymer cages. This can be explainable by an analogy of a series arrangement of resistors and capacitances. In case, when the retainer is made of metal, it can short-circuit all bearings' balls, while a non-conductive polymer cage can behave capacitive only. By separating the bearings' volume in three areas, a capacitance-resistance-capacitance-combination can be represented, while a polymer cage bearing leads to a three-times-capacitance combination as shown in **Figure 8**. Due to the inverse proportionality to the sum of the reciprocals of the individual capacitances, the capacitance of the metal retainer bearing must be higher. Another consequence of

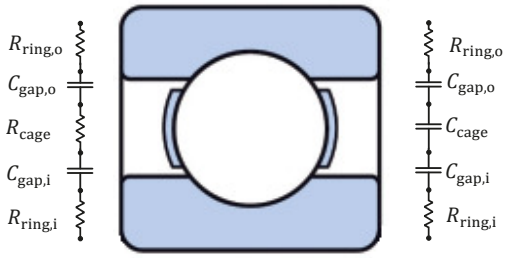

Figure 8: Reproduction of the electrical properties of a bearing with either metal (left) or plastic retainer (right) with electrical elements

the metal cage is its provision of an additional conductive surface on which charges can accumulate. This can cause a change in the charge and electric field distribution in the capacitor, thus affecting its electrical properties.

3.3 Oil type influence

In **Figures 9 and 10** the measurement result of the capacitance for the metal cage bearing type SKF 6011 and SKF 61813 with no additional load are shown. When sprayable lubricants are used, the plots initially show a decrease in capacitance as the shaft speed increases. This is explainable by the flow of the lubricants into the ball-ring contact, resulting in a build-up of a lubricant film. Consequently, a thicker film height causes a smaller capacitance. As the shaft speed increases further, the lubricant is forced out of the contact zone, leading to starvation effects, as explained in [1]. This phenomenon describes the lubrication film becoming thinner due to the flow of the lubrication out of the contact zone. By reason of the viscosity, the lubricant cannot flow back into the contact zone fast enough. The contact zone starves of lubrication and as consequence, the capacitance increases due to a low lubrication film height h_0. This effect is clearly observed in the study of the SKF 6011 in **Figure 10** with the HHS Lube lubricant, where above 3200 rpm, no capacitance, but a resistive impedance is measured. This indicates that the viscosity of this lubricant is too high, preventing sufficient lubrication in the contact zone. The lubricant HHS 2000, which is very low viscous

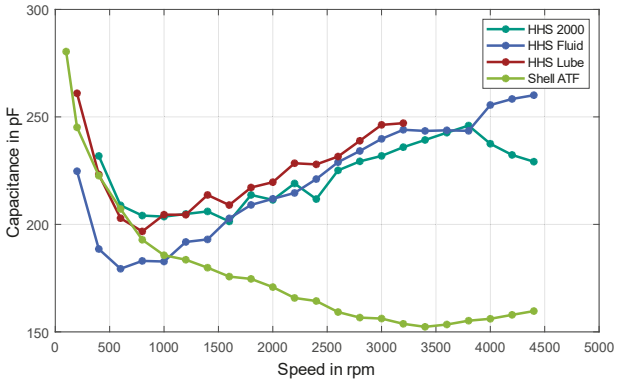

Figure 9: Capacitance measurements of the SKF 61813 by variation of the lubricants

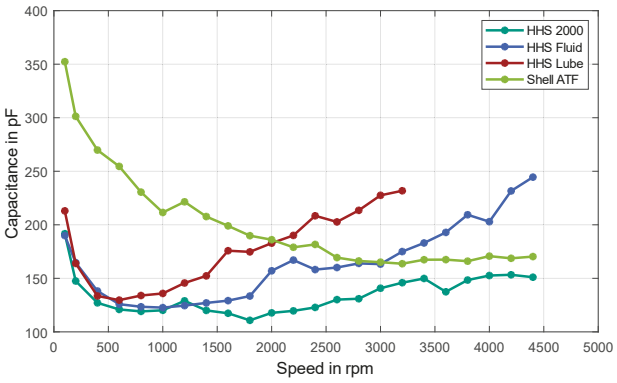

Figure 10: Capacitance measurements of the SKF 6011 by variation of the lubricants

instead, and therefore allows the oil to flow back into the contact zone easily, resulting in a uniform lubrication film at lower speeds and a flatter increase in capacitance. By comparing the measurement results for both bearing types, the difference in magnitude for the bearings, already explained in **Section 3.1**, can be observed here again. Another salience can be found in the capacitance for the SKF 6011 bearing, since it shows wider divergence, while the curves for the SKF 61813 remain closer together. This can be explained by the number of balls, their diameter, and radial clearance. Since the SKF 6011 has a more spacious volume for the lubricants, dynamic effects can arrange somehow freely. These findings suggest that the variation in lubrication type does not exert the primary influence on the capacitance. The behavior for the low-viscous Shell ATF is very different from the higher viscous sprayable lubricants, depictable in **Figures 9 and 10**. Although, the capacitance of the bearing drops initially as seen for the other lubricants, but then it remains on an almost constant plateau. This behavior can be explained by the very low viscosity and the very low oil film height already at low shaft speeds. Increasing the shaft speed does not change the lubrication condition in the contact zone exceptionally. The lower capacitance values for the low viscous lubricants can be explained by their permittivity. According to [12], lubricants with higher viscosity tend to have higher permittivity val-

ues. Since the permittivity directly correlates with capacitance, it follows that the capacitance must be higher for lubricants of high viscosity.

3.4 Axial load influence

The consideration of an unloaded bearing is described in **Section 3.1** in combination with the Shell ATF. The unloaded scenario, where bearings solely support the own weight of the motors' structure, represents just a relatively small fraction of all load conditions over the drives' operational lifetime. In **Figure 11,** the curves show the capacitance measurement results for different axial loads over speed without any additional radial loads. Based on the analytical **Formula (2),** it is evident that an increase in the axial load must result in a corresponding higher capacitance level. This is because higher loads result not only in a larger Hertzian contact area A_{Hertz}, but also lead to a reduction in the lubricant film thickness h_0 within each rolling contact. The effect is quantified in the dimensionless parameter $\bar{W}$ of a single rolling element by **Formula (3)**. As the measurement result shows, there is no direct proportionality between the increase in axial load and the increase in capacitance. This effect is explainable due to the fact, that an elevated load causes both, an expansion in the Hertzian contact area A_{Hertz} and a reduction in the lubricants' film thickness h_0 within each rolling contact.

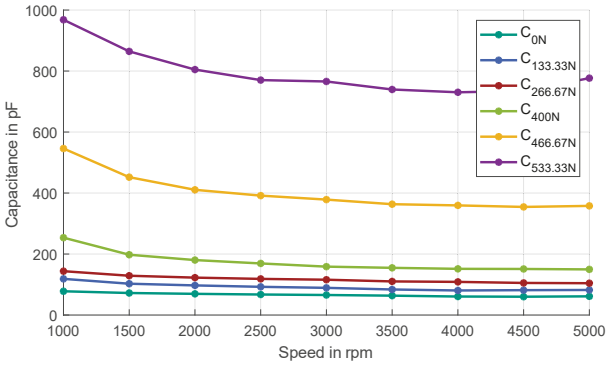

Figure 11: Capacitance measurements by variation of axial loads

3.5 Radial load influence

The measured curves in **Figure 12** under the influence of additional radial loads are similar to those of the axial loads. By increasing the radial load, the capacitance must rise, since also in this case, higher loads lead to a reduction in the lubricant film height h_0, simultaneously to the increase of the Hertzian contact area A_{Hertz}. Not directly intuitive is the fact, that the influence of axial loads on the capacitance is much higher than radial loads. Regarding the analytical **Formula (1)**, the reasoning is possible. Since the Hertzian surface area A_{Hertz} increases under load and the raceways in ball bearings are curvilinear, the relevant contact surface after an imprint of axial load increases faster than the normal contact area after radial loads. Due to the elasto-hydrodynamic pressure, an insulated lubrication film thickness in radial direction can be built up straightforward because an equilibrium in load distribution is reached.

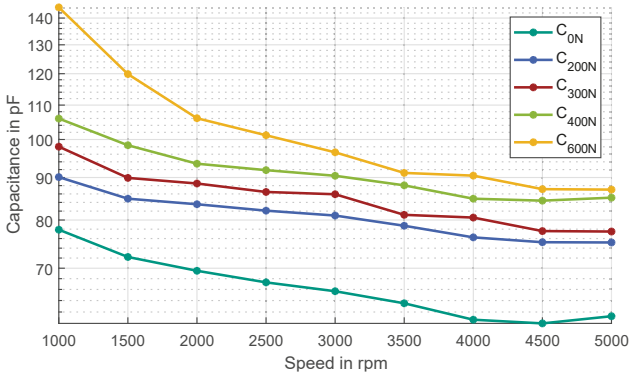

Figure 12: Capacitance measurements by variation of radial loads

4 Summary and Outlook

The experimental setup in the present paper reveals many crucial influences on the bearings' behavior under high-frequency excitation. The study shows that the prediction of the bearings' capacitance is not easily possible, since many different parameters, already depictable by the empirically determined formulas from literature, are influencing. The measurement results presented in this paper investigated various parameters, including speed variations, radial and axial loads, different types of lubricants, or the bearings' retainer material separately, to understand each parameter change isolated. With the help of these separate in-depth investigations, the way towards a more general analytical determination of the bearings' capacitance is aimed. The main difficulties in the capacitance determination arise from dynamic effects. Not only the temperature increase but also highly dynamic effects, such as starvation effects or vibrations of the structure can influence the measurement results.

In a following study, combined load cases must be investigated, since an isolated load case, e.g. pure radial or axial load is rarely in a motor's operation life. As an outlook, impedance measurement can be also used to monitor the damage condition of ball bearings. Changes in the impedance can indicate potential faults or wear in the bearings but also lubrication issues or misalignments. Furthermore, the lubrication conditions, by means of the elasto-hydrodynamic regime in the rolling contact, which can be either a metallic contact, an insulated lubrication film, or every condition between these two extreme states, can be identified by impedance measurements. Lastly, by extending the bearing test bench with a current source with high current magnitudes, a breakdown of the bearings' capacitance can be enforced, and therefore lifetime test with defined damage targets or when corrugated patterns start arising can be determined. Moreover, with this test setup, the deduction of the breakdown voltage of the lubricants under realistic motor operating conditions is possible.

5 Literature

[1] S. Scheuermann, “Development of a Bearing Test Bench to Investigate Root Causes of Bearing Current Damages”, IEMDC 2023, San Francisco, conference contribution, June 2023.

[2] A. Dyson, H. Naylor & A. R. Wilson, “The Measurement of Oil-Film Thickness in Elastohydrodynamic Contacts,” Proceedings of the Institution of Mechanical Engineers, Conference Proceedings, vol. 180, no. 2, pp. 119–134, 1965.

[3] A. W. Crook, “The Lubrication of Rollers II. Film Thickness with Relation to Viscosity and Speed,” Philosophical Transactions of the Royal Society A: Mathematical, Physical and Engineering Sciences, vol. 254, no. 1040, pp. 223–236, 1961.

[4] P. Brüser, “Untersuchungen über die elastohydrodynamische Schmierfilmdicke bei elliptischen Hertzschen Kontaktflächen,” Dissertation, Fakultät für Maschinenbau und Elektrotechnik, Technische Universtität Braunschweig, Braunschweig, 1972.

[5] E. C. Wittek, ”Charakterisierung des Schmierungszustandes im Rillenkugellager mit dem kapazitiven Messverfahren“, Gottfried Wilhelm Leibniz Universität Hannover, Hannover, 2017.

[6] SKF. https://www.skf.com/uk/products/rolling-bearings/ball-bearings/deep-groove-ball-bearings/productid-6011 (last visit: 28.06.2023)

[7] SKF. https://www.skf.com/uk/products/rolling-bearings/ball-bearings/deep-groove-ball-bearings/productid-61813 (last visit: 28.06.2023)

[8] Würth. HHS 2000 Safety Data Sheet. https://pim.wurth.ca/Technical/SDS_893.106.pdf (last visit: 28.06.2023)

[9] Würth. HHS Technical Data in overview. https://www.klickparts.com/out/media/124266.pdf (last visit: 28.06.2023)

[10] Würth. HHS Lube Safety Data Sheet. https://shop.wohlfeil.de/media/pdf/28/c9/39/Sicherheitsdatenblatt_HHSLube.pdf (last visit: 28.05.2023)

[11] Shell. Spirax S6 ATF D971. https://www.shell-livedocs.com/data/published/en/e18a9d59-95f6-4f7e-b29e-aa598d9fbbcd.pdf (last visit: 28.06.2023)

[12] H. Sun, Y. Liu, J. Tan “Research on Testing Method of Oil Characteristic Based on Quartz Tuning Fork Sensor”, Applied Sciences. 2021; 11(12):5642. https://doi.org/10.3390/app11125642